Electronics and Electrical Engineering

AIMS Electronics and Electrical Engineering, 8(1): 28–52.
DOI: 10.3934/electreng.2024002
Received: 14 December 2023
Revised: 06 February 2024
Accepted: 20 February 2024
Published: 23 February 2024

http://www.aimspress.com/journal/ElectrEng

Research article

Torque and d-q axis current dynamics of an inverter fed induction motor drive that leverages computational intelligent techniques

Shaswat Chirantan* and Bibhuti Bhusan Pati

Department of Electrical Engineering, Veer Surendra Sai University of Technology, Burla, Sambalpur, 768018, India

*** Correspondence:** Email: shaswat.chirantan443@gmail.com.

Abstract: Emphasizing the significance of Model Predictive Control (MPC) in modern optimization of control systems, the proposed research distinctively highlights its predictive prowess through the application of current state variables and well-structured mathematical models. We introduced a Predictive Current Control (PCC) strategy applied to a Three-Phase Inverter-fed Induction Motor (IM), with a particular focus on the Sequential Model methodology. The Sequential Model MPC algorithm employed a cost functional approach, predicated on the square of the discrepancy between reference and stator-measured currents of the IM in d-q reference frame. This method, implemented and tested in both MATLAB/Simulink and Python environments, utilized a minimization principle to guide the switching states of the inverter, thereby ensuring the accuracy of voltage signals for the induction motor. The projected study further included a comparative analysis of the electromagnetic torque, load currents, rotor speed, and angle deviations derived from the Sequential Model with those obtained through the Ant Colony Optimization (ACO) and Nelder-Mead methods. The results distinctly illustrated the robust adaptability of the Sequential Model methodology, outperforming the ACO and Nelder-Mead techniques in certain aspects such as minimum current errors, better speed regulations, and rotor angle trajectories.

Keywords: predictive current control; model predictive control; induction motor; sequential model; ant colony optimization; Nelder-Mead method

List of symbols

(i_{sd}, i_{sq})	Components of stator current in ***(d, q)*** reference frame
(u_{sd}, u_{sq})	Components of stator voltage in ***(d, q)*** reference frame
S_a, S_b, S_c	Switching States of the inverter
R_s, R_r	Winding resistance offered to stator and rotor
L_s, L_r	Winding inductance of stator and rotor
L_h	Mutual inductance
J_m	Moment of inertia
F_d	Friction viscous gain
Z_p	Number of pole pairs
$\omega_s, \omega_m, \omega_e$	Stator, Mechanical and Electrical speed
T_e, T_L	Electromagnetic and Load Torque
V_{DC}	DC Bus Voltage
V_{aN}, V_{bN}, V_{cN}	Phase Voltages
Ψ_{rd}	Rotor flux of direct axis
σ	Leakage Factor
τ_s, τ_r	Stator and Rotor Time constant
$i_{sd}(t_{i+1}), i_{sq}(t_{i+1})$	Predicted values of current in d-q frame,
i_{sd}^*, i_{sq}^*	Desired values of current in d-q frame.
δt	Sampling Interval

Abbreviations: MPC: Model predictive control; PCC: Predictive current control; IM: Induction motor; CCS: Continous control set; FCS: Finite control set; SEQ: Sequential model; ACO: Ant colony optimization; NM: Nelder-Mead method; PMSM: Permanent magnet sysnchronous machine; PWM: Pulse width modulation; GA: Genetic algorithm; GSA: Gravitational search algorithm

1. Introduction

Model Predictive Control (MPC) has proven to be highly effective in managing the switching of power converters, synchronous and induction machine drives, and various power system parameters. Its flexibility, robustness, and swift dynamic responses have inspired numerous predictive control algorithms. Depending on their operational dynamics and control actions, MPC topology can be classified into analogous mode or continuous control set (CCS) and discrete mode. Studies such as [1] have proposed predictive current control schemes for power converters and electrical drives, exemplifying the CCS-MPC algorithm with a receding horizon control principle, forward Euler approximation, a cost function for the discrete time load model of PMSM (permanent magnet synchronous motor), and induction motor for the switching states of the inverter.

In recent years, predictive control methods have become a pivotal area of interest for induction motor drives due to their superior dynamic response and simplified implementation over traditional methods. Wang et al. first introduced integral FCS predictive current control of induction motor drives, providing a basis for improving dynamic response and static error performance [2]. Subsequent research by Wang et al. introduced the application of PID and predictive control methods using MATLAB/Simulink, affirming the advantages of these predictive control approaches [3]. However, this work lacked an in-depth exploration of practical implementation challenges. Advancements in this field continued with Odhano et al. and Ahmed et al. who explored direct flux

and current vector control [4], as well as Finite Control Set-Model Predictive Speed Control [5]. These studies validated the control principles and applications for high-performance drive systems. With respect to the aforesaid literatures, predictive models of induction motor drive can also be implemented for advancement in control strategies and design prospectives [6–9].

Further, the exploration of the Sequential Model in this context can add more depth to the understanding of steady-state errors. Sequential Models, often represented mathematically as a series of layers, each of which transforms its input data according to specific predefined rules, perform complex transformations on raw data to generate a result. The application of the Sequential Model involves the calculation of each layer's output as the input to the next, aiming to minimize steady-state error in a systematic, step-by-step manner.

In addition, the Ant Colony Optimization (ACO) is applied for its efficient search capabilities. ACO algorithms are represented mathematically by a pheromone model that updates trail levels as per a local and global updating rule. This rule is based on the quality of solutions found the shorter the path, the higher the pheromone trail, guiding the 'ant colony' to potentially optimal solutions. Thus, in controlling the flux dynamics of an Induction Motor, Ant Colony Optimization can help direct the search towards an optimal or near-optimal solution.

To assess the effectiveness of these control strategies, we have compared the Sequential Model [10–16] and Ant Colony Optimization (ACO) [17–19] with the Nelder-Mead simplex method [20–23], known for its simplicity and efficiency in multi-dimensional optimization problems. Further, computational intelligence techniques such as Genetic Algorithm [24], Particle Swarm Optimization [25,26] and Gravitational Search Algorithm [27,28] can also be applied for optimal tuning of induction motor drives.

Apart from this, studies on torque control & speed regulations of induction machine incorporate the concept of direct torque control scheme [29–32]. The findings demonstrate the unique advantages and disadvantages of each approach in the context of induction motor drives. Despite the continuous evolution of control strategies and the introduction of novel techniques, the deployment of model predictive control in power electronics continues to augment the robustness, flexibility, and speed of the designed control frameworks. This research strives to augment this foundation, investigating the potential of Sequential Models in the context of induction motor drives.

The article is structured to allow an in-depth understanding of the applied methodologies. Section 2 begins with an overview of related studies and research literature, providing a comprehensive context for exploration. Advancing further, Section 3 details the dynamic model, inverter topology, control strategies, and essential algorithms implemented for the forecasted controllers of an Induction Motor (IM) drive. This part also delves into the framework and application of the Sequential model (SEQ), Ant Colony Optimization (ACO) and Nelder Mead (NM) method. Section 4 is dedicated to the presentation and discussion of the responses of torque, currents, and speeds concerning step alterations of various proposed control measures. Following this, Section 5 offers a comparative study on the designed Model Predictive Controls (MPCs) with an emphasis on their dynamic characteristics related to torque and current. The article concludes with Section 6, encapsulating the major findings from the research and listing relevant references.

2. Related review and research gap

The application of Sequential Models (SEQ) in induction motor drives were explored by researchers in [10–15], where the Sequential Model was used to simulate and analyze the dynamic response of induction motor drives. They demonstrated that the Sequential Model, with its

step-by-step analytical approach, could accurately predict the dynamic performance of the drives, thereby improving their efficiency and reliability. The integration of Ant Colony Optimization (ACO) in induction motor drives has also been a point of interest. Studies demonstrated in [17–19] introduced the use of ACO for optimizing the control of induction motors. They demonstrated the ability of ACO to quickly converge to optimal or near-optimal solutions, enhancing the overall performance of the motor drives. In the subsequent research by the authors [17–19], the efficacy of ACO was affirmed, showcasing its robustness in handling high-performance drive systems. Further, studies in [18] contrasted the application of ACO with current-based and flux/torque-based model predictive control methods, favoring ACO due to its superior efficiency in reducing current ripple and enhancing dynamic response. More recently, a comprehensive analysis among the advanced control strategies: Field Oriented Control, Direct Torque Control, Sequential Models, and Ant Colony Optimization, revealing the dominance of ACO and Sequential Models in terms of performances. Postulation of Nelder-Mead method in machine drive system [20–23] for optimal control has also significant impact while scrutinizing the desired activities. Moreover, a deeper exploration by researchers into the potential of these techniques in power electronics revealed significant strides in predictive control scheme applications.

3. Modelling and control techniques

The operational principle of Model Predictive Control (MPC) is fundamentally based on predicting and controlling a variable of interest over a finite horizon, mathematically represented as N. For inverter states, expressed as X_{in}, without the use of any Pulse Width Modulation (PWM) methods. The control system design incorporates eight potential inverter state combinations, represented as (x_1, x_2 …., x_8), which serve as constraints in our optimization problem. By integrating the load model, represented as m_load, into the analysis, we can generate better predictions for future behavior of system variables, hence leading to the term model predictive. The optimization technique operates following the principle of receding horizon control. In a constraint-free Sequential Model MPC method, the system behaves similarly to a discrete time deadbeat feedback control system. Here, the controller gain k changes over time, provided the closed-loop poles are positioned at the origin of the complex plane. To improve the steady-state behavior of the standard Sequential Model MPC method, an integral action is introduced through a cascade control structure with two gain parameters k_d and k_q for both direct & quadrature axis respectively. The objective function J_obt in a standard Sequential Model MPC method, aimed for minimization, is defined as the deviations between the predicted and desired outputs which is similar to that of current error in d-q reference frame. In contrast, the purpose of the objective function in the Sequential Model MPC method is directly related to the sampling period, denoted as δt . This correlation introduces a temporal element to the control strategy, further refining the predictive capability of the model.

3.1. Adaptive approach to MPC

Model Predictive Control (MPC) operates on the foundation of a finite-horizon control principle, characterized by its continuous prediction and dynamic re-calibration. This dynamic process is guided by the controller, the epicenter of the MPC system, which computes control signals for a predetermined future time frame, termed the predictive horizon. As each moment passes, this finite window of time adapts, assimilating an upcoming time span and discarding the elapsed one. Using projected system output, the MPC generates a control sequence exclusive to the current sampling

time, with subsequent sampling intervals prompting modifications based on freshly measured variables. A visual illustration of this process can be seen in Figure 1, where various trajectories depict key signals. The desired path, or reference signal, is represented by a red line, while the controlled signal, derived from measurements and adjustments at the time instant 'k', is marked in green. The groundwork for future predictions, provided by the past measured variable, is traced by a yellow curve. At each current state, 'k', 'k+1', 'k+2', and so forth, the MPC formulates distinct control sequences for the corresponding prediction horizons, manifesting a cyclical, real-time strategy for effective predictive control.

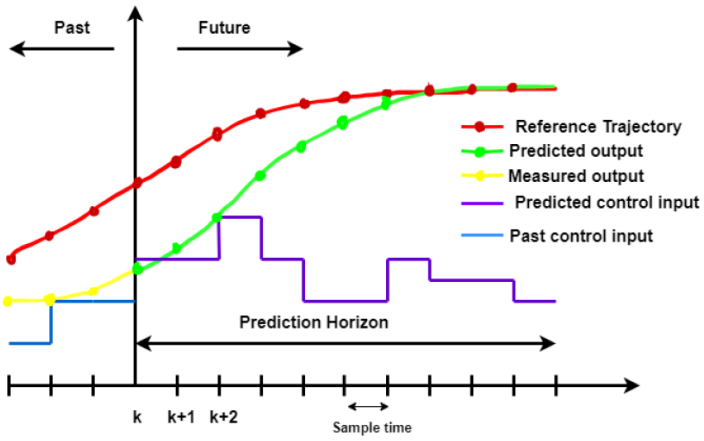

Figure 1. Prediction horizon trajectory for MPC methodology.

In this study, we focus on simplifying inverter states optimization, which eliminates the requirement for any Pulse Width Modulation (PWM) approach. We consider eight combinations of inverter states as constraints for designing the control mechanism. A load model is used to predict the future dynamics of the variables, hence the term Model Predictive Control (MPC). The optimization methodology operates based on the principle of receding horizon control. Essentially, a constraint-free MPC method aligns with a discrete time deadbeat feedback control system, where the controller gain changes over time, given that the closed-loop poles are located at the origin of the complex plane. To improve the steady-state performance of the traditional MPC method, a cascade control structure that introduces an integral action is employed. In a typical MPC method, the objective function for minimization is simply the squared difference between the predicted and measured currents in the d-q reference frame. However, in the sequential model in MPC method, it is explicitly associated with the sampling time δt.

3.2. Induction motor's dynamic framework

For our experimental setup within a simulation framework, we considered a squirrel cage induction motor as a case study. The dynamics of current and torque are represented by the following mathematical equations, based on the d-q reference frame, as detailed in [3]. As the proposed control scheme is based on stator current modulation and thereby evaluating the machine dynamics, it is necessary to modeled the IM in terms of d-q axis currents. Stator current dynamics can be represented in Equations (1) and (2).

$$\frac{di_{sd}}{dt} = -\frac{1}{\tau_\sigma} i_{sd} + \omega_s i_{sq} + \frac{k_r}{r_\sigma \tau_\sigma \tau_r} \varphi_{rd} + \frac{1}{r_\sigma \tau_\sigma} u_{sd} \tag{1}$$

$$\frac{di_{sq}}{dt} = -\omega_s i_{sd} - \frac{1}{\tau_\sigma} i_{sq} - \frac{k_r}{r_\sigma \tau_\sigma} \omega_e \varphi_{rd} + \frac{1}{r_\sigma \tau_\sigma} u_{sq} \tag{2}$$

The relation between stator and rotor speed of the induction motor in terms of mutual inductance, rotor time constant and d-q axis current can be defined in Eqs (3) and (4) respectively.

$$\omega_s = \omega_e + \frac{L_h}{\tau_r} \tag{3}$$

$$\omega_s = \omega_e + \frac{1}{\tau_r} \frac{i_{sq}}{i_{sd}} \tag{4}$$

Where

i_{sd} & i_{sq} are the measured currents in d-axis, q-axis, expressed in Ampere (A),
u_{sd} & u_{sq} are the measured voltages in d-axis, q-axis, expressed in Volt (V),
ω_s, ω_e are the angular speed of the stator and rotor, expressed in rad/sec,
φ_{rd} = Rotor flux of d-axis (Wb).

Equations (1) and (2) define the overall current dynamics of the designed IM model, and the parameters used in the dynamic equations illustrate the IM kinetic characteristics. The fraction of the magnetic flux utilization is determined by the leakage factor and expressed as:

Leakage factor: $$\sigma = 1 - \frac{L_h^2}{L_s L_r} \tag{5}$$

In order to study the current responses in both the stator and rotor winding, we need to define the term time constant and those can be presented in Eqs (6) & (7), respectively.

Stator time constant: $$\tau_s = \frac{L_s}{R_s} \tag{6}$$

Rotor time constant: $$\tau_r = \frac{L_r}{R_r} \tag{7}$$

The coefficients used in the current dynamic equation of modeled IM are denoted as follow:

Coefficients: $$k_r = \frac{L_h}{L_r} \tag{8}$$

$$r_\sigma = R_s + R_r k_r^2 \tag{9}$$

$$\tau_\sigma = \frac{\sigma L_s}{r_\sigma} \tag{10}$$

The torque generated due to magnetic field, commonly known as electromagnetic torque, is proportional to the product of direct axis rotor flux φ_{rd} and quadrature axis stator current i_{sq}, which is expressed as:

$$T_e = \frac{3}{2} Z_p \frac{L_h}{L_r} \varphi_{rd} i_{sq} \tag{11}$$

The functionality of T_e is such that it creates a relative motion between stator and rotor by the application of load torque, T_L (Eq (12)). As it also depends on q-axis current characteristics, the dynamic behavior of the machine can be predicted by analyzing Eq (11).

The mechanical parametrics of the induction motor need to be consider and derived from the general motor equation for rotation, which is given as follows,

$$J_m \frac{d\omega_m}{dt} + f_d \omega_m = T_e - T_L \tag{12}$$

where, $\omega_m(t)$ is the mechanical velocity of the rotor($\omega_m = \frac{\omega_e}{Z_p}$), J_m is the inertia of the motor, and

f_d is the friction coefficient.

In order to exemplify the rotor speed response to the corresponding step input current, the speed dynamics equation can be obtained by putting Eq (12) in Eq (11), & represented as,

$$\frac{d\omega_m}{dt} = \frac{-f_d}{J_m}\omega_m + \frac{3}{2}\frac{Z_p L_h}{L_r J_m}\varphi_{rd} i_{sq} - \frac{T_L}{J_m} \tag{13}$$

The velocity of the rotor in the electrical field can be extracted from Eq (13) and expressed as,

$$\frac{d\omega_e}{dt} = \frac{-f_d}{J_m}\omega_e + \frac{3}{2}\frac{Z_p^2 L_h}{L_r J_m}\varphi_{rd} i_{sq} - \frac{Z_p T_L}{J_m} \tag{14}$$

The physical and technical parameters defined, and used earlier in the IM model have been considered and mentioned in Table 1 below for system performance evaluation.

Table 1. 3-Φ IM model parameters [3].

Parameters	**Values**
Winding resistance offer to Stator (R_s)	11.2 Ohms
Winding resistance offer to Rotor (R_r)	8.3 Ohms
Winding inductance offer by Stator (L_s)	0.6155 Henrys
Winding inductance offer by Rotor (L_r)	0.6380 Henrys
Mutual inductance of Machine (L_h)	0.57 Henrys
Moment of inertia (J_m)	0.00176 kg-meter square
Friction viscous gain (f_d)	0.00038818 newton meter/radian/second
Number of pole pair (Z_p)	2 Nos

3.3. Tri-Phase inverter design and analysis

We consider a 3-φ invertor, which convert 520V to 3-φ AC, For the study, we considered a squirrel cage type induction motor, the physical parameters of which are provided in Table 1. The operation of the inverter is based on a non-linear discrete time system, functioning in a 180° mode with seven output states and eight configuration states. To facilitate simplicity in our modeling and mathematical computations for the simulation, we have disregarded the saturation voltage of the Insulated-Gate Bipolar Transistor (IGBT) and the forward voltage drop of the diode. The schematic power circuit as the voltage source, inverter to the 3-φ IM is given below in Figure 2.

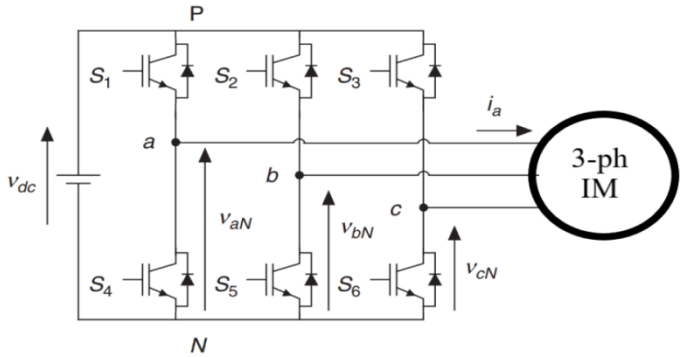

Figure 2. P ower circuit of VSI fed 3-Φ IM.

The switching state for conversions is carryout with the reference of the gating signalsS_a, S_b, S_c , and represented as follows [1]:

$$S_a = \begin{cases} 1, \text{if } Switch_1 \text{ on and } Switch_4 \text{ off} \\ 0, \text{if } Switch_1 \text{ off and } Switch_4 \text{ on} \end{cases}$$

$$S_b = \begin{cases} 1, \text{if } Switch_2 \text{ on and } Switch_5 \text{ off} \\ 0, \text{if } Switch_2 \text{ off and } Switch_5 \text{ on} \end{cases}$$

$$S_c = \begin{cases} 1, \text{if } Switch_3 \text{ on and } Switch_6 \text{ off} \\ 0, \text{if } Switch_3 \text{ off and } Switch_6 \text{ on} \end{cases}$$

The principle of space vector modulation is employed in the context of voltage vectors corresponding to optimal switching states. The creation of switching states culminates in eight voltage vectors, as indicated in Table 2. These vectors can be forecasted by deploying Eq (15) as demonstrated below:

$$v = \frac{2}{3} V_{dc} (S_a + aS_b + a^2 S_c) \tag{15}$$

Where, a = $e^{-j(2\pi/3)} = -\frac{1}{2} + j\frac{\sqrt{3}}{2}$, with a phase displacement of 120°, between any two phases.

Table 2. Switching states with corresponding voltage vectors.

S_a	S_b	S_c	Voltage Vector (v)
0	0	0	$\overrightarrow{v_0} = 0$
1	0	0	$\overrightarrow{v_1} = \frac{2}{3} v_{dc}$
1	1	0	$\overrightarrow{v_2} = \frac{1}{3} v_{dc} + j \frac{\sqrt{3}}{3} v_{dc}$
0	1	0	$\overrightarrow{v_3} = -\frac{1}{3} v_{dc} + j \frac{\sqrt{3}}{3} v_{dc}$
0	1	1	$\overrightarrow{v_4} = -\frac{2}{3} v_{dc}$
0	0	1	$\overrightarrow{v_5} = -\frac{1}{3} v_{dc} - j \frac{\sqrt{3}}{3} v_{dc}$
1	0	1	$\overrightarrow{v_6} = \frac{1}{3} v_{dc} - j \frac{\sqrt{3}}{3} v_{dc}$
1	1	1	$\overrightarrow{v_7} = 0$

The uncomplicated mathematical representation of the three-phase inverter circuit, as shown in Figure 3, outlines the generation of output voltages (phase to neutral) in response to applied switching signals. The ideal operation of predictive algorithms results in the switching states outlined above.

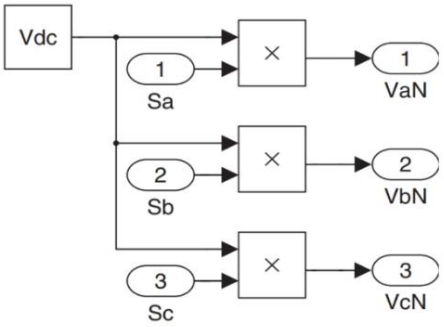

Figure 3. Voltage output of VSI [1].

3.4. Advanced predictive current regulation

The proposed predictive current control algorithm incorporates the optimization mechanism as follows:

Step 1: At each state, measure the load current, i(t), and obtain the reference current, $i^*(t_i+1)$, from the outer control loop.

Step 2: Evaluate and predict the value of the load current for the upcoming sampling interval, $i(t_i+1)$. Remember to account for different voltage vectors in the prediction.

Step 3: Calculate the cost function, J, which quantifies the error between the reference and predicted currents. This calculation should be performed for each upcoming sampling frame, taking the corresponding voltage vector into account. The cost function, J, can be represented as:

$$J=\{i_d^*(t_i)-i_d(t_{i+1})\}^2+\{i_q^*(t_i)-i_q(t_{i+1})\}^2 \quad (16)$$

Step 4: Generate switching state signals that aim to minimize the current error, as computed by the cost function. These signals should be factored into the system control process.

Step 5: Repeat Steps 1 to 4 at each sampling interval, establishing a closed-loop control system.

This algorithm considers both the preceding load current value and the subsequent current state to predict 7 diverse states, resulting in 8 distinct configurations for the operation of the inverter switching. For each discrete state, the predicted current value is calculated and compared to the reference current to minimize error and fluctuations. This calculation is required for all 8 states, as presented in the table above, with the associated errors recorded. The optimal operational states are then supplied to the inverter functioning as the voltage source. The process flow of the aforementioned steps is illustrated in Figure 4.

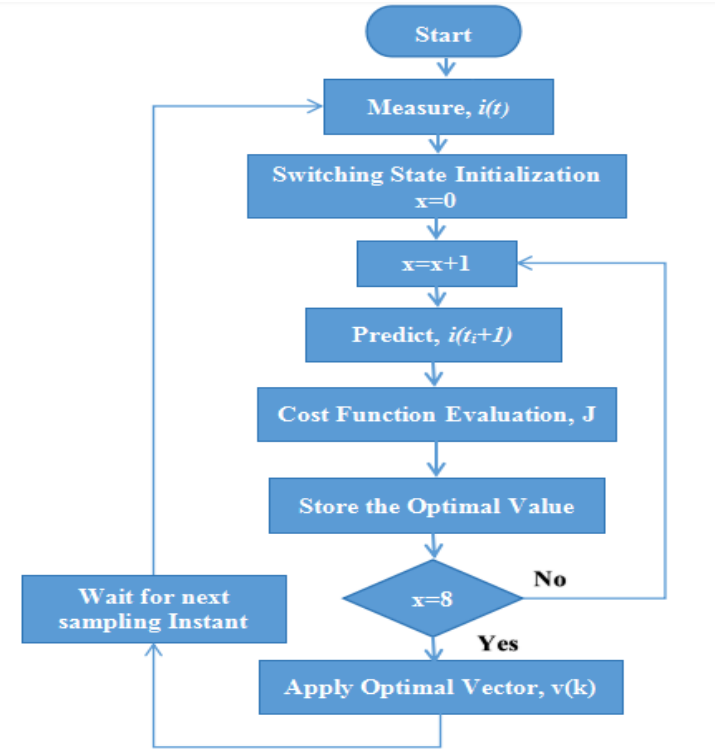

Figure 4. Flow chart for a predictive current control scheme.

3.5. SEQ-MPC for induction motor

Regarding generalization of equations, predicted load currents in d-q frame for sampling time $\mathbf{t_i}$ can be derived from forward Euler Approximations [1]. Dynamic equations of d-q axis currents have been stated earlier in Eqs (1) & (2). Further upgrades in current trajectories at various time instants for a predefined sampling interval can be charactrized by Eqs (17) and (18). These mathematical expressions predict the one step ahead characteristics of injected current signals w.r.t the specified cost function.

$$\frac{di_{sd}(t)}{dt} \approx \frac{i_{sd}(t_{i+1}) - i_{sd}(t_i)}{\delta t} \tag{17}$$

$$\frac{di_{sq}(t)}{dt} \approx \frac{i_{sq}(t_{i+1}) - i_{sq}(t_i)}{\delta t} \tag{18}$$

Where δt is assumed as the sampling time interval,
$i_{sd}(t_{i+1})$ And $i_{sq}(t_{i+1})$ are predicted values of current in d-q frame, ${i_{sd}}^*$and ${i_{sq}}^*$ are the desired values of current in d-q frame.

Now, using Eqs (17) & (18) in Equations (1) & (2) respectively, the discrete differential equations become the difference equations and can be represented as follows:

$$i_{sd}(t_{i+1}) = i_{sd}(t_i) + \delta t\left(-\frac{1}{\tau_\sigma} i_{sd}(t_i) + \omega_s i_{sq}(t_i) + \frac{k_r}{r_\sigma \tau_\sigma \tau_r} \varphi_{rd}(t_i) + \frac{1}{r_\sigma \tau_\sigma} u_{sd}(t_i)\right) \tag{19}$$

$$i_{sq}(t_{i+1}) = i_{sq}(t_i) + \delta t\left(-\omega_s i_{sd}(t_i) - \frac{1}{\tau_\sigma} i_{sq}(t_i) - \frac{k_r}{r_\sigma \tau_\sigma} \omega_e(t_i)\, \varphi_{rd}(t_i) + \frac{1}{r_\sigma \tau_\sigma} u_{sq}(t_i)\right) \tag{20}$$

The discretized prediction equations corresponding to Eqs (19) and (20) are also presented in matrix form.

$$\begin{bmatrix} i_{sd}(t_{i+1}) \\ i_{sq}(t_{i+1}) \end{bmatrix} = (\mathrm{I} + \delta t A_m(t_i)) \begin{bmatrix} i_{sd}(t_i) \\ i_{sq}(t_i) \end{bmatrix} + \Delta t B_m \begin{bmatrix} u_{sd}(t_i) \\ u_{sq}(t_i) \end{bmatrix} + \begin{bmatrix} \frac{k_r \Delta t}{r_\sigma \tau_\sigma \tau_r} \varphi_{rd}(t_i) \\ -\frac{k_r \Delta t}{r_\sigma \tau_\sigma} \omega_e(t_i)\, \varphi_{rd}(t_i) \end{bmatrix} \quad (21)$$

Where,
I is a 2*2, identity matrix and

$$A_m(t_i) = \begin{bmatrix} -\frac{1}{\tau_\sigma} & \omega_s(t) \\ -\omega_s(t) & -\frac{1}{\tau_\sigma} \end{bmatrix} \quad : \qquad B_m = \begin{bmatrix} \frac{1}{r_\sigma \tau_\sigma} & 0 \\ 0 & \frac{1}{r_\sigma \tau_{\sigma q}} \end{bmatrix}$$

3.5.1. System dynamics in SEQ-MPC

The dynamic system modeling of proposed Sequential Model has been illustrated as follows:

1. System Dynamics: The state of our system at a future time step, denoted as $k+1$, is dependent on the current state k and the control action u at the current time step k. This relationship is represented by the equation, $x(k+1) = Ax(k) + Bu(k) + w(k)$. additionally, there exists an inherent process noise term $w(k)$ that is assumed to follow a normal distribution with zero mean and covariance, Q.
2. Measurement Model: Measurements of the system state z are also influenced by the true system state, captured by the equation $z(k) = Hx(k) + v(k)$. Here $v(k)$ represents the measurement noise term which, like the process noise, is typically assumed to follow a normal distribution but with covariance, R.
3. MPC Optimization Problem: The heart of our Sequential Model Predictive Control (SEQ-MPC) lies in its ability to solve an optimization problem that determines the optimal sequence of control actions. This optimization seeks to minimize the difference between the predicted and actual system states, across a prediction horizon, as represented by the equation:

$$\min u(k), \ldots, u(k+N)$$
$$\{ E[\, x(k+N+1)' S x(k+N+1) + \Sigma\{ x(k+i)' Q x(k+i) + u(k+i-1)' R u(k+i-1) \}\,] \} \quad (22)$$

In this equation, N is the prediction horizon, $E[.]$ denotes the expectation (since we're considering the statistical case), and `'` denotes the transpose operation. `S`, `Q`, and `R` are weight matrices for the state and control actions. The optimization is subject to constraints which maintain the system dynamics, represented as

$$x(k+i+1) = Ax(k+i) + Bu(k+i) + w(k+i),\ i = 0, \ldots, N. \quad (23)$$

By integrating these concepts, the SEQ-MPC provides a robust control methodology that is adaptive to system noise and provides optimal control actions to regulate the system behavior. Please note that this implementation will require a strong understanding of stochastic optimization and control theory due to its probabilistic nature.

Table 3. Algorithm for proposed sequential model.

Algorithm: SEQ approach	
Step-1:	Initialize SEQ: Set up the structure of the motor dynamics with n layers, and initialize the weights $W_{[i]}$ and biases $b_{[i]}$ for layer *i* randomly.
Step-2:	Forward propagation: Given the motor parameters at time *t*, $x_{[t]}$, calculate the output of each layer i using the equations:
Step-3:	Compute loss: Calculate the loss $L_{[t]}$ between the prediction $a[n]$ and the target output $y_{[t]}$ using the chosen loss function.
Step-4:	Backward propagation: Compute the derivative of each layer's pre-activation value with respect to its weights and biases. These derivatives are calculated using the chain rule of calculus and the derivatives of the activation functions and the loss function.
Step-5:	Update weights and biases: Adjust the weights and biases using the derivatives calculated in the previous step and the learning rate.
Step-6:	Repeat steps 2-5: Continue the training process for a certain number of epochs, or until the network's performance on a validation set stops improving.
Step 7:	Evaluate the model for get the best fitness value.

The receding horizon control principle is used here that predicts one step ahead value from the feedback parameters such as $i_{sd}(t_i)$, $i_{sq}(t_i)$, ω_e and θ_e from 3-ph IM model. The objective function is calculated based on the above feedback values, parameters of 3-ph IM model and the pair of $u_{sd} - u_{sq}$ values. Seven sets of objective function are calculated based on seven pairs of $u_{sd} - u_{sq}$ values. The index value is 0 or 7, will be determine with the previous states of the inverter. The switching combinations and corresponding voltage vectors imposed in SEQ-MPC technique are shown in Table 4.

Table 4. Switching states and voltage vectors of SEQ-MPC block.

S_a	S_b	S_c	Voltage Vector (v)	V_{an}	V_{bn}	V_{cn}
0	0	0	$\overrightarrow{v_0}$	$-\frac{V_{dc}}{2}$	$-\frac{V_{dc}}{2}$	$-\frac{V_{dc}}{2}$
1	0	0	$\overrightarrow{v_1}$	$\frac{V_{dc}}{2}$	$-\frac{V_{dc}}{2}$	$-\frac{V_{dc}}{2}$
1	1	0	$\overrightarrow{v_2}$	$\frac{V_{dc}}{2}$	$\frac{V_{dc}}{2}$	$-\frac{V_{dc}}{2}$
0	1	0	$\overrightarrow{v_3}$	$-\frac{V_{dc}}{2}$	$\frac{V_{dc}}{2}$	$-\frac{V_{dc}}{2}$
0	1	1	$\overrightarrow{v_4}$	$-\frac{V_{dc}}{2}$	$\frac{V_{dc}}{2}$	$\frac{V_{dc}}{2}$
0	0	1	$\overrightarrow{v_5}$	$-\frac{V_{dc}}{2}$	$-\frac{V_{dc}}{2}$	$\frac{V_{dc}}{2}$
1	0	1	$\overrightarrow{v_6}$	$\frac{V_{dc}}{2}$	$-\frac{V_{dc}}{2}$	$\frac{V_{dc}}{2}$
1	1	1	$\overrightarrow{v_7}$	$\frac{V_{dc}}{2}$	$\frac{V_{dc}}{2}$	$\frac{V_{dc}}{2}$

The phase to neutral voltages of each phase can be defined w.r.t switching states and DC input voltage of inverter as below:

$$\begin{bmatrix} V_{an} \\ V_{bn} \\ V_{cn} \end{bmatrix} = \begin{bmatrix} S_a - \frac{1}{2} \\ S_b - \frac{1}{2} \\ S_c - \frac{1}{2} \end{bmatrix} \mathrm{V_{dc}} \tag{24}$$

3.6. A-SEQ-MPC: A statistical approach

The Sequential Model utilizes an underpinning principle similar to traditional control methods, but it follows a distinct control action. In this Sequential Model approach, the objective function incorporates variables in terms of data transformation rules applied layer by layer. Each layer in the Sequential Model performs a specific transformation on its input data, thus formulating the output as an input to the next layer. This layer by layer processing aids in generating a result from complex transformations of raw data.

Hence, the Sequential Model constructs the optimal control signals through this layered feedback control framework.

$$\begin{bmatrix} u_{sd}(t_i)^{opt} \\ u_{sq}(t_i)^{opt} \end{bmatrix} = K_{seq} \left(\begin{bmatrix} {i_{sd}}^*(t_i) \\ {i_{sq}}^*(t_i) \end{bmatrix} - \begin{bmatrix} i_{sd}(t_i) \\ i_{sq}(t_i) \end{bmatrix} \right) \tag{25}$$

Where, K_{seq} is the gain matrix of the controller and can be extracted from Eq (21) as:

$$K_{seq}(t_i) = (\delta t^2 \mathrm{B_m^T B_m})^{-1} \ \mathrm{B_m^T} \delta t \ (\mathrm{I} + \delta t A_m(t_i)) \tag{26}$$

Further simplifying by putting the matrix form of A_m & $\mathrm{B_m}$,

$$K_{seq}(t_i) = \begin{bmatrix} \frac{r_\sigma \tau_\sigma}{\delta t}(1 - \frac{\delta t}{\tau_\sigma}) & \omega_s(t_i) r_\sigma \tau_\sigma \\ -\omega_s(t_i) r_\sigma \tau_\sigma & \frac{r_\sigma \tau_\sigma}{\Delta t}(1 - \frac{\delta t}{\tau_\sigma}) \end{bmatrix} \tag{27}$$

Using integral action in discrete time control system, Equation (25) can be modified as:

$$\begin{bmatrix} u_{sd}(t_i)^{opt} \\ u_{sq}(t_i)^{opt} \end{bmatrix} = K_{seq}(t_i) \begin{bmatrix} \frac{k_d}{1-q^{-1}} \ ({i_{sd}}^*(t_i) - i_{sd}(t_i)) \\ \frac{k_q}{1-q^{-1}} \ ({i_{sq}}^*(t_i) - i_{sq}(t_i)) \end{bmatrix} - \begin{bmatrix} i_{sd}(t_i) \\ i_{sq}(t_i) \end{bmatrix} \tag{28}$$

Where *'k_d'* and 'k_q' are the value of integral block parameters used for current error at both d-axis and q-axis respectively, $0 < k_d \leq 1$ and $0 < k_q \leq 1$ and $\frac{1}{1-q^{-1}}$ represents functionality of an integrator.

Now at sampling time t_i the optimum control signals are calculated as

$$\begin{bmatrix} u_{sd}(t_i)^{opt} \\ u_{sq}(t_i)^{opt} \end{bmatrix} = \begin{bmatrix} u_{sd}(t_{i-1})^{opt} \\ u_{sq}(t_{i-1})^{opt} \end{bmatrix} + K_{seq}(t_i) \begin{bmatrix} K_d \ ({i_{sd}}^*(t_i) - i_{sd}(t_i)) \\ K_q \ ({i_{sq}}^*(t_i) - i_{sq}(t_i)) \end{bmatrix} - K_{seq}(t_i) \begin{bmatrix} \delta i_{sd}(t_i) \\ \delta i_{sq}(t_i) \end{bmatrix} \tag{29}$$

The modified objective function for SEQ-MPC is given as

$$J_K = \frac{\delta t^2}{(r_\sigma \tau_\sigma)^2} \ (u_{sd}(t_i)^K - u_{sd}(t_i)^{opt})^2 + \frac{\delta t^2}{(r_\sigma \tau_\sigma)^2} \ (u_{sq}(t_i)^K - u_{sq}(t_i)^{opt})^2 \tag{30}$$

The objective function is calculated for each control having an index value denoted by K = 0, 1, 2, 6. For the control set associated with the index value that yields the minimum objective function, a

corresponding switching pulse is generated for the inverter. A representation of the SEQ-MPC for an Induction Motor (IM) can be viewed in Figure 5.

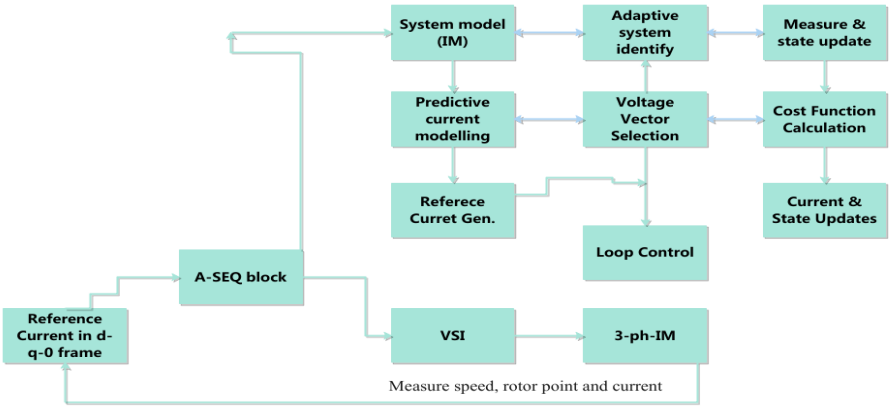

Figure 5. Structure of SEQ-MPC for IM.

The Sequential Model Predictive Control (SEQ-MPC) approach, specifically designed for a three-phase induction motor, integrates integral gain parameters and optimal voltage vectors. It is graphically represented in Figure. 6, depicting the structure of the predictive current controller in the d-q reference frame, while illustrating the practical application of Equation (28). When these integral gain parameters are modified, Equation (29) is derived, further enhancing the evaluation of the integral FCS control mechanism. Integral gain parameters, k_d and k_q are set at 0.1 as per previous research [3], although further exploration could involve varying these parameters within the range from 0 to 1. In Figure 6, the control system operates by adaptively identifying a suitable system model for the induction motor based on input-output data. It measures motor currents, updating the model state after applying the selected voltage vector, while also acquiring reference values for the motor currents from the outer control loop. The system then predicts the motor currents for the subsequent sampling interval, taking into account the different voltage vectors applied by the Voltage Source Inverter (VSI). A cost function is computed to quantify the error between the references and predicted motor currents, alongside the control effort. The system subsequently selects the voltage vector that minimizes this cost function, using it to regulate the VSI. Current measurements and state updates are performed after applying the chosen voltage vector. The process is continuously iterated, establishing a closed-loop adaptive control system.

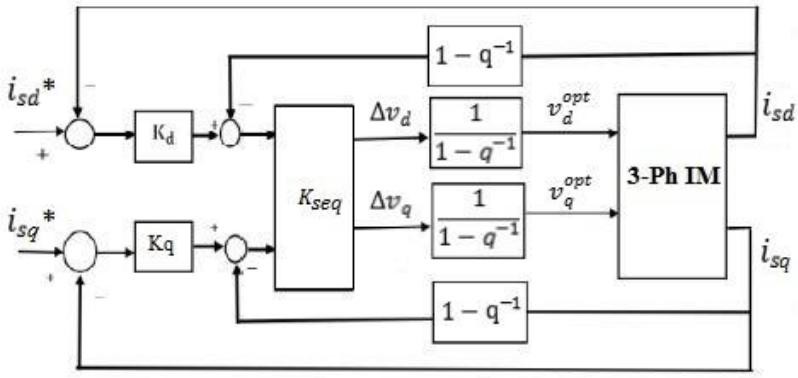

Figure 6. Architecture of proposed SEQ-MPC.

3.7. Organizing ACO and NM for induction motor

The application of metaheuristic algorithms like Sequential Modelling (SEQ) and Ant Colony Optimization (ACO) has come to the forefront in induction motor control, heralding a new age of innovative and efficient system optimization. Sequential Modeling breaks complex systems into manageable steps, enabling an orderly and incremental understanding of system dynamics, which is especially beneficial in the intricate landscape of induction motor control. Complementing this, Ant Colony Optimization, a probabilistic technique inspired by ant behavior, uses artificial 'ants' to navigate the solution space, gradually building towards an optimal solution based on the pheromone trails of their peers. This mimicry of natural robustness allows the algorithm to explore extensive solution spaces and hone in on optimal or near-optimal results, while avoiding the pitfalls of local minima. Both techniques, owing to their stochastic nature, are highly effective for handling the inherent nonlinearities of induction motor control. Nevertheless, the success of Sequential Modelling and Ant Colony Optimization heavily relies on the fine-tuning of their respective algorithmic parameters, underscoring the need for meticulous attention to these details in the quest for optimal outcomes.

The Nelder-Mead method and Ant Colony Optimization (ACO) have emerged as significant strategies in intelligent control methodologies for induction motor drives. The Nelder-Mead method, a direct search method, is particularly useful for optimizing control systems. It works by refining a simplex, a polytope of n+1 vertices in n dimensions, to converge on the optimal solution. This makes it exceptionally suitable for problems like induction motor control, where it is important to minimize parameters such as energy consumption or optimize performance metrics like torque and speed control. On the other hand, ACO emulates the behavior of ants seeking a path between their colony and a food source. In this context, the "food source" represents the optimal solution to a control problem, while the "ants" represent individual solutions to the problem. As the algorithm iterates, the "pheromone trail" strengthens along more optimal solutions, guiding the algorithm towards the best control parameters. However, similar to other optimization algorithms like the Genetic Algorithm (GA) and the Gravitational Search Algorithm (GSA), the performance of the Nelder-Mead method and ACO highly depends on the unique characteristics of the induction motor and the specifics of the control problem. This necessitates precise tuning and adaptation of these methodologies for achieving optimal control of the induction motor drive. Parameters considered for NM and ACO are presented in Table 5.

Table 5. Parameter constraints used for NM and ACO.

ACO Parameters	**NM Parameters**
Number of Ants (pop_size) = 100	Number of vertices = [0,0] - [10/400,10/400]
Maximum Iterations (ngen) = 100-500	Reflection coefficient (alpha) = 1.0
Lower and Upper bounds = [0,0]- [10/400,10/400]	Expansion coefficient (gamma) = 2.0
Pheromone evaporation coefficient, rho = 0.5	Contraction coefficient (rho) = 0.5
Initial Pheromone level = 0.1	Shrinkage coefficient (sigma) = 0.5
Number of elite ants = 5	Maximum Iterations (ngen) = 500

3.7.1. Applying algorithm on motor dynamics

Ant Colony Optimization and Nelder-Mead Methods are applied to the modeled IM according to the mentioned logics in Table 6. The illustrated algorithms of the proposed ACO and NM project the desired optimal activities by calculating the predefined objective function mentioned in Equation (16). Further, the generation of appropriate switching states stimulate the injection of optimal voltage vectors to the induction motor. This process continues until the achievement of most ideal condition of operation. Based on these criteria, the yearned parameters such as current, torque, and speed responses of the IM can be evaluated with respect to the step input signal.

Table 6. ACO & NM optimization algorithm.

	ACO Algorithm		**NM Algorithm**
Step-1:	Define the model of the induction motor. The search space consists of all feasible configurations of the motor parameters.	Step-1:	Define the model of the induction motor and identify the parameters to be optimized.
Step-2:	Initialize a population of n artificial ants, placing them randomly in the search space. Each ant represents a specific configuration of the motor parameters.	Step-2:	Initialize a simplex of n+1 vertices X[i] in n dimensions, each representing a specific configuration of motor parameters.
Step-3:	Define the fitness function based on the motor parameters such as efficiency, torque, speed, etc. For instance, *fitness = efficiency * speed – torque.*	Step-3:	Define the fitness function as before, e.g., *fitness = efficiency * speed – torque.*
Step-4:	Each ant I probabilistically selects the next configuration j using the formula mentioned in the previous response, considering the pheromone intensity and desirability of the path.	Step-4:	Order the vertices from best to worst according to f(X[i]) and compute the centroid C of the n best vertices.
Step-5:	After all ants have completed their paths, update the pheromones on the paths using the formula provided earlier.	Step-5:	Follow the reflection, expansion, contraction, and shrinkage steps mentioned earlier to generate a new simplex.
Step-6:	If the termination conditions are not met, go back to Step 4.	Step-6:	If the termination conditions are not met, go back to Step 4.

4. Results and discussions

The three-phase induction motor with specified parameters mentioned earlier has been modeled and executed with SEQ, ACO and NM control algorithms applied to inverter circuit. The dynamic

characteristics of currents, torque, and angular speed of IM have been analyzed for different predictive schemes implemented here. Overall simulation and sampling time are set to be 0.2s and 10μs, respectively.

4.1. Dynamic current analysis

The reference input current in d-q axis is depicted in Figure 7. From the input current plot, it can be seen that d-axis current is taken to be a constant value of i_{sd} = 0.8 A and q-axis current is considered to be a step signal of amplitude i_{sq} = 3 A and changes to 1 A at 0.1 sec.

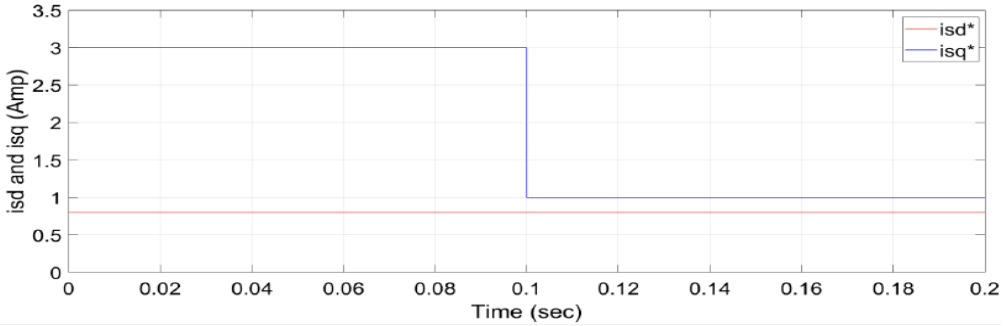

Figure 7. Three phase reference current in d-q frame.

Considering the d-q axis currents and change in rotor angle (θ), the desired currents' characteristics in three-phase quantities also shift at a specific instant. These currents can be regarded as a reference for the currents in the upcoming execution cycle and assumed as the standard for all proposed estimations. The output currents in d-q forms procured by Sequential Model, NM, and Ant Colony Optimization methods are demonstrated in Figures 8 and 9, respectively.

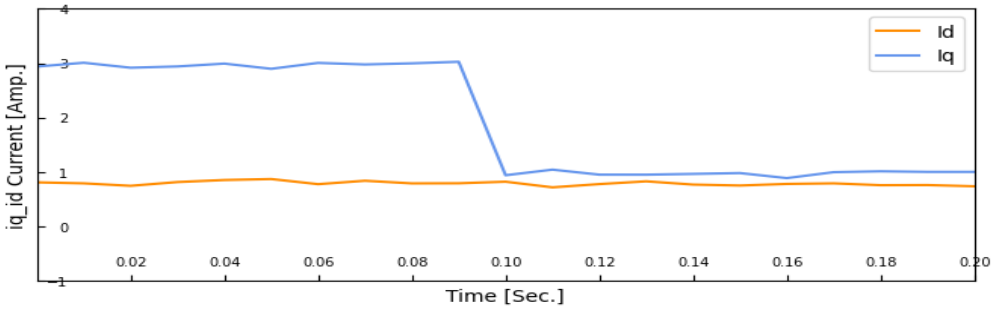

Figure 8. d-q axis currents of SEQ method.

In examining rotor angle (θ) dynamics and d-q axis currents, the application of the Sequential Model and Ant Colony Optimization plays a pivotal, meta-heuristic role. The complexity of these dynamics lies in the immediate influence that variations in θ exert on the characteristics of the currents in three-phase quantities. For the ensuing execution cycle, a key presupposition is proposed: The currents identified by the model will serve as the reference. This benchmark stems from the outcomes derived from the implementation of the Sequential Model, NM, and Ant Colony Optimization techniques. To provide a more concrete understanding of these methodologies' impacts, the resultant currents are graphically depicted. Figure 8, demonstrates the output currents in d-q form,

a result of implementing the Sequential Model, while Figure 9(a) and 9(b), exhibit the d-q form of output currents, a consequence of the Nelder Mead and Ant Colony Optimization technique respectively. Consequently, these figures offer a clearer understanding of the impact of the NM and Ant Colony Optimization in the modelling of currents, along with a comparison with the SEQ method.

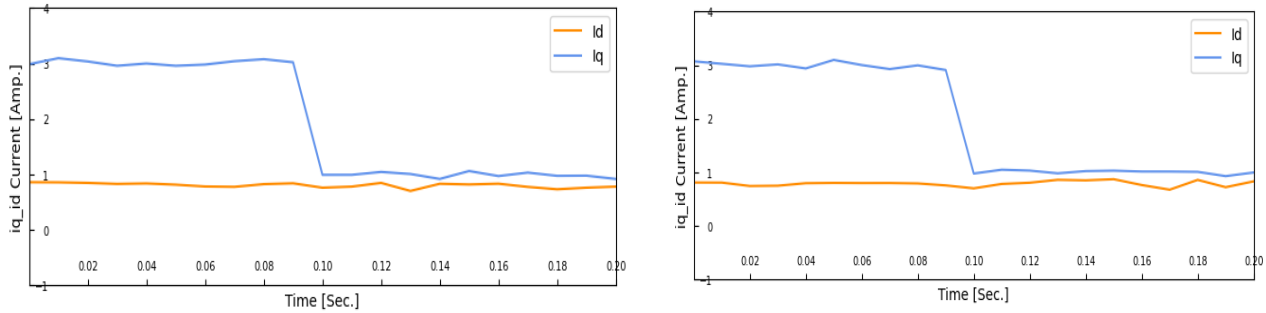

(a) NM method (b) ACO method

Figure 9. d-q axis current characteristics of proposed control algorithms.

4.2. Torque and speed dynamic analysis

From Eq (11), it can be clearly adopted that electrical torque output (T_e) is a function of quadrature axis current and rotor flux of an induction motor. As a result, the behavior of q-axis current controls the torque characteristics. The plots of reference load torque and output torque obtained from SEQ predictive control schemes are depicted in Figure 10(a) and 10(b), respectively. The applied load torque to the induction motor drive is a step signal of amplitude 2Nm and step change occurs to 1Nm at time 0.1second

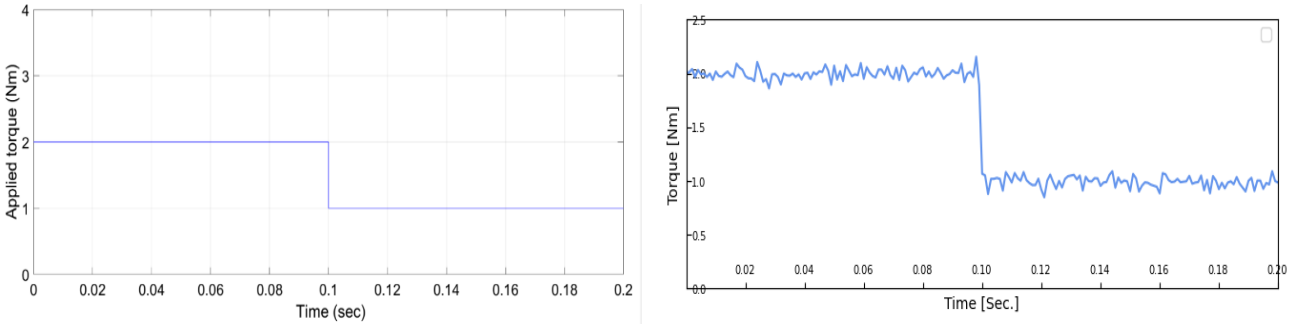

(a) Applied load torque (b) Torque output of SEQ-MPC method

Figure 10. Load torque characteristics.

It is well understood that parameters such as electromagnetic torque output, quadrature axis current, rotor flux, and angular speed are interdependent in the context of an induction motor. Modifications in any of these parameters will result in direct alterations in the others, thereby impacting the motor's performance. By controlling the current, we can effectively manage the torque and the angular speed of the motor can be regulated in tandem with other dependent parameters, as mathematically formulated by Eqs (13) and (14). By applying the Sequential Neural Network model, we can control these parameters, as illustrated in Figure 10, which depicts the torque characteristics

corresponding to step changes in load torque and q-axis current. In addition to these, the Ant Colony Optimization and Nelder-Mead optimization techniques also provide a robust approach to optimize and control these interdependent parameters of the induction motor, offering another efficient solution for motor control. Figures 11(a) and 11(b) show the torque output of the NM method and ACO method, respectively.

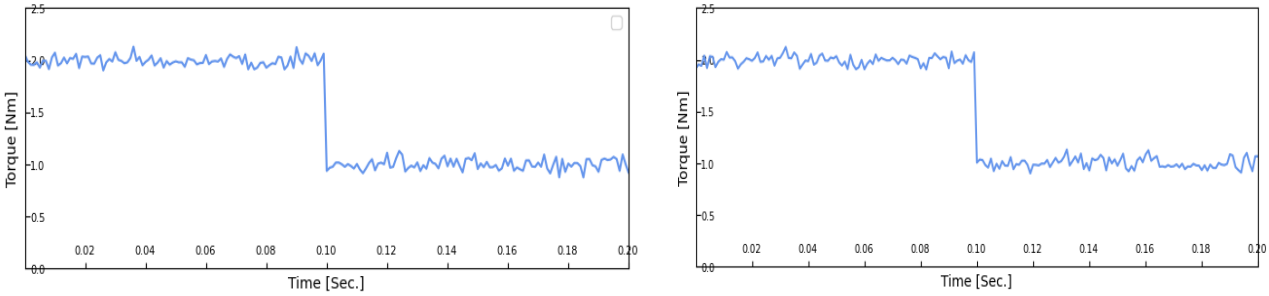

(a) Torque output of NM method

(b) Torque output of ACO method

Figure 11. Predicted torque output of implemented optimization algorithms.

Our prior examinations have underscored the intricate interdependence of various parameters in defining the performance of an induction motor. One subtle shift can trigger a cascade of changes, intricately linking current manipulation to torque control and indirectly to the angular speed of the motor, as vividly illustrated in Figure 12. However, this mechanism is not standalone; it operates within a complex web of interdependent parameters, a relationship distinctly captured by Eqs (13) and (14). The deployment of advanced algorithms such as Sequential Models, Ant Colony Optimization (ACO), and Nelder-Mead optimization can elucidate these intricate dynamics, providing a comprehensive exploration of the induction motor's angular speed response to respective adjustments in load torque and q-axis current. However, it is crucial to emphasize that while the Sequential, ACO, and Nelder-Mead methods yield considerable insights into the motor's performance, the graphical demonstrations in Figure 12, portraying the angular speed characteristics realized through these strategies, highlight the potential for further optimization. Thus, these observations underscore the paramount importance of synergistic coordination of interrelated parameters to enhance motor performance using these advanced algorithms.

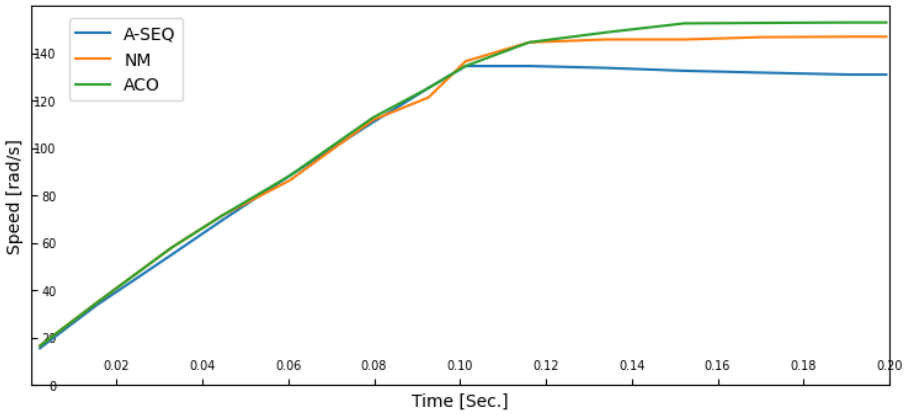

Figure 12. Angular speed of the SEQ-MPC, ACO, and NM methods.

The evaluation of the induction motor drive's optimum performance is conducted by examining the model outputs for currents, torque, angular speed, and rotor angle (as depicted in Figure 13). The dynamic of current is studied using a reference step signal of the quadrature axis current. The electromagnetic torque output of the machine follows suit with the applied step load torque as the output torque is a function of the q-axis current and rotor flux, as defined by Eq (11). As the rotor position angle updates with every time instant, the corresponding angular speed also alters. The step responses for current, torque, and speed obtained by SEQ control strategies are illustrated here. Ripple quantities in the current and torque output can be discerned from the output responses. It can be stated that these ripples are less pronounced in the SEQ-MPC when compared to Ant Colony Optimization and Nelder-Mead Method. A performance comparison is carried out based on the model outputs of the implemented MPC strategies, focusing on aspects such as absolute current errors, torque characteristics, speed and rotor angle responses with respect to the applied step changes.

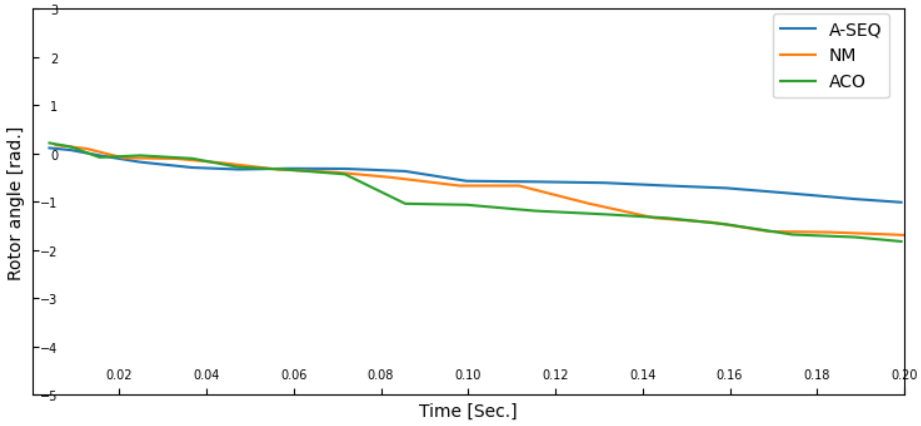

Figure 13. Rotor angle of SEQ-MPC, ACO, NM method.

In the quest for peak performance, an in-depth examination of the devised induction motor drive model brings to light the importance of several variables - currents, torque, angular speed, and perhaps most crucially, the rotor angle (θ). Each of these factors plays a crucial part in the intricate dynamics of motor operation. A particularly captivating element arises from the study of current dynamics, which is conducted via a reference step signal of the quadrature axis current. Interestingly, this signal exerts a significant impact on the output of the machine's rotor angle, illustrating the complex interplay within the system. Additionally, every change to the rotor position angle prompts a corresponding modification in the angular speed, underscoring the fine equilibrium within these dynamics. Notably, the application of the SEQ-MPC method yields a heightened level of control over these dynamics, superior to that afforded by ACO, Nelder-Mead. This pivotal observation accentuates the remarkable effectiveness of the adaptive approach in both optimizing rotor angle control and enhancing the overall performance of the induction motor drive, thereby establishing it as a favorable strategy for motor control.

5. Comparability of proposed optimal controllers

Simulations of SEQ-MPC, NM, and ACO models are implemented with a sampling time of 10 microseconds. Two major factors that determine the characteristic results are sampling time and

integral gain constants, k_d and k_q. For higher value of integral gains, the current trajectories will overshoot with a good performance in steady state. If we keep the integral gain low, dynamic overshoot can be compensated. Here, the value of integral gains are taken as 0.1. Sampling time does not strongly affect dynamic performance, as its effect is mostly a steady state ripple. With a higher sampling time, the ripple present are more; hence, the sampling time needs to be reduced. However, the computational burden and switching loss of the inverter are restricting the sampling time to fall below a certain value. Therefore, a compromise is made between the allowable ripple and computational time as well as switching loss. The current errors obtained by the proposed optimization techniques are shown in Table 7.

Table 7. Absolute errors of d-q axis currents measured by applied intelligent techniques.

SI. No.	Applied Optimization Technique	Absolute Current Error(Amp)		Total Error(Amp)
		$\lvert I_{dRef} - I_{dMeas} \rvert$	$\lvert I_{qRef} - I_{qMeas} \rvert$	
1	**SEQ-MPC**	0.1145	0.2826	0.3971
2	**NM**	0.4459	0.3755	0.8214
3	**ACO**	0.3665	1.0792	1.4457

As the objective of the applied control techniques is to stimulate the inverter operation by optimizing the defined cost function, it is of utmost priority to select the foremost approach by considering the least current error. Thus, it is intelligibly making a selection towards the Sequential Neural Model method for optimum operation of the induction motor drive. A better representation and comparison of total current errors can be depicted in Figure 14.

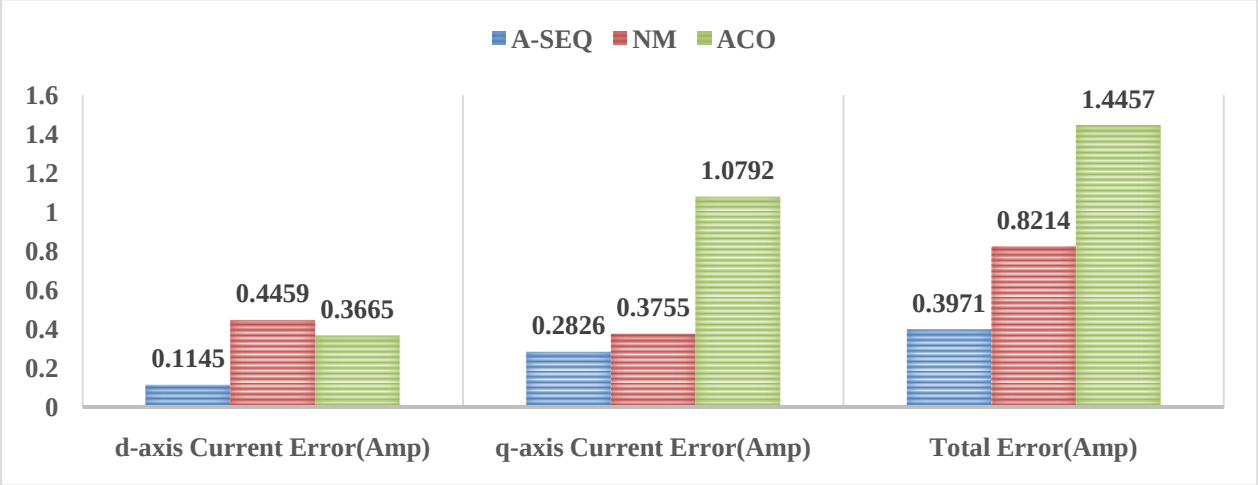

Figure 14. d-q axis current errors by SEQ-MPC, NM & ACO.

6. Conclusions

Induction motors find significant application across various industries, including traction, process, production, and mining, owing to their crucial roles in the creation of electromagnetic

torque and the dynamics of inverter-fed voltages. Among various speed and torque control methodologies, such as conventional PI, PID, and hysteresis controllers, the sequential model (SEQ-MPC) has emerged as a preferred choice due to its predictive accuracy, capability of handling non-linear loads, steady state error minimization, and fast response to transient disturbances. The technique is further enriched with the incorporation of Nelder-mead (NM) and Ant Colony Optimization (ACO), which add an extra dimension to the analysis of 3-phase Induction Motor (IM) dynamics. Through manipulation of the reference current in the d-q axis and the reference load torque as step functions, the dynamic behavior of the 3-phase IM can be scrutinized more closely. Even though NM and ACO have showcased prominent strengths in IM control, the proposed SEQ-MPC model displays superior performance across multiple facets. Maintaining a control strategy analogous to motor dynamics intrinsically minimizes steady-state errors, enhances slew rates, and provides improved trajectories concerning the step input signal. The adaptive and flexible traits of MPC methods earmark these controllers as superior alternatives in the contemporary control scenario. SEQ-MPC outperforms Nelder-Mead and ACO with respect to absolute current error compensation and sustainable current and speed responses, thereby reinforcing its position as a favored option for the designed asynchronous motor model. The extrapolation of this predictive control approach has the potential to bring about significant advances in applications such as electric vehicles, facts devices, and diverse power system control measures.

Use of AI tools declaration

The authors declare that they have not used Artificial Intelligence (AI) tools in the creation of this article.

Acknowledgments

The authors would like to thank Veer Surendra Sai University of Technology, Burla, Sambalpur, India for facilitating this work.

Conflict of interest

The authors declare that there are no conflicts of interest in this paper.

References

1. Rodriguez J, Cortes P (2012) *Predictive Control of Power Converters and Electrical Drives*, John Wiley & Sons Ltd, United Kingdom. https://doi.org/10.1002/9781119941446
2. Wang L, Gan L (2014) Integral FCS predictive current control of induction motor drive. *IFAC Proceedings Volumes* 47: 11956–11961. https://doi.org/10.3182/20140824-6-ZA-1003.00753
3. Wang L, Chai S, Yoo D, Gan L, Ng K (2015) *PID and predictive control of electrical drives and power converters using MATLAB/Simulink*, JohnWiley & Sons. https://doi.org/10.1002/9781118339459

4. Odhano S, Bojoi R, Formentini A, Zanchetta P, Tenconi A (2017) Direct flux and current vector control for induction motor drives using model predictive control theory. *IET Electr Power Appl* 11: 1483–1491. https://doi.org/10.1049/iet-epa.2016.0872
5. Ahmed AA, Koh BK, Kim JS, Lee YI (2017) Finite control set-model predictive speed control for induction motors with optimal duration. *IFAC Papers On Line* 50: 7801–7806. https://doi.org/10.1016/j.ifacol.2017.08.1056
6. Wang J, Wang F (2020) Robust sensor less FCS-PCC control for inverter-based induction machine systems with high-order disturbance compensation. *J Power Electron* 20: 1222–1231. https://doi.org/10.1007/s43236-020-00113-8
7. Fereidooni A, Davari SA, Garcia C, Rodriguez J (2021) Simplified Predictive Stator Current Phase Angle Control of Induction Motor with a Reference Manipulation Technique. *IEEE Access* 9: 54173–54183. https://doi.org/10.1109/ACCESS.2021.3070790
8. Rodriguez J, Garcia C, Mora A, Flores-Bahamonde F, Acuna P, Novak M, et al. (2021) Latest Advances of Model Predictive Control in Electrical Drives—Part I: Basic Concepts and Advanced Strategies. *IEEE T Power Electr* 37: 3927–3942. https://doi.org/10.1109/TPEL.2021.3121532
9. Rodriguez J, Garcia C, Mora A, Davari SA, Rodas J, Valencia DF, et al. (2021) Latest advances of model predictive control in electrical drives—Part II: Applications and bench marking with classical control methods. *IEEE T Power Electr* 37: 5047–5061. https://doi.org/10.1109/TPEL.2021.3121589
10. Tang Y, Xu W, Dong D, Liu Y, Ismail MM (2022) Low-Complexity Multistep Sequential Model Predictive Current Control for Three-Level Inverter-Fed Linear Induction Machines. *IEEE T Ind Electron* 70: 5537–5548. https://doi.org/10.1109/TIE.2022.3192688
11. Yang X, Zhang L, Xie W, Zhang J (2019) Sequential and Iterative Distributed Model Predictive Control of Multi-Motor Driving Cutterhead System for TBM. *IEEE Access* 7: 46977–46989. https://doi.org/10.1109/ACCESS.2019.2908388
12. Wang T, Wang Y, Wang X, Han M, Rodr ́guez J, Zhang Z (2021) A Statistics-Based Dynamic Sequential Model Predictive Control for Induction Motor Drives. *2021 IEEE International Conference on Predictive Control of Electrical Drives and Power Electronics (PRECEDE)*, 513–518, https://doi.org/10.1109/PRECEDE51386.2021.9681001
13. Vodola V, Odhano S, Norambuena M, Garcia C, Vaschetto S, Zanchetta P, et al. (2019) Sequential MPC Strategy for High Performance Induction Motor Drives: a detailed analysis. *2019 IEEE Energy Conversion Congress and Exposition (ECCE)*, 6595–6600. https://doi.org/10.1109/ECCE.2019.8912708
14. Vodola V, Odhano S, Garcia C, Norambuena M, Vaschetto S, Zanchetta P, et al. (2019) Modulated Model Predictive Control for Induction Motor Drives with Sequential Cost Function Evaluation. *2019 IEEE Energy Conversion Congress and Exposition (ECCE)*, 4911–4917. https://doi.org/10.1109/ECCE.2019.8911870
15. Wang Y, Zhang Z, Huang W, Kennel R, Xie W, Wang F (2019) Encoderless Sequential Predictive Torque Control with SMO of 3L-NPC Converter-fed Induction Motor Drives for Electrical Car Applications. *2019 IEEE International Symposium on Predictive Control of Electrical Drives and Power Electronics (PRECEDE)*, 1–6. https://doi.org/10.1109/PRECEDE.2019.8753238

16. Kerboua A, Kelaiaia R (2023) Fault Diagnosis in an Asynchronous Motor Using Three-Dimensional Convolutional Neural Network. *Arab J Sci Eng*, 1–19. https://doi.org/10.1007/s13369-023-08025-y
17. Yin Z, Du C, Liu J, Sun X, Zhong Y (2018) Research on Autodisturbance-Rejection Control of Induction Motors Based on an Ant Colony Optimization Algorithm. *IEEE T Ind Electron* 65: 3077–3094. https://doi.org/10.1109/TIE.2017.2751008
18. Mahfoud S, Derouich A, Iqbal A, El Ouanjli N (2022) ANT-colony optimization-direct torque control for a doubly fed induction motor: An experimental validation. *Energy Rep* 8: 81–98. https://doi.org/10.1016/j.egyr.2021.11.239
19. Dhieb Y, Yaich M, Guermazi A, Ghariani M (2019) PID controller tuning using ant colony optimization for induction motor. *J Electr Syst* 15: 133–141.
20. Essa MS, Elhosseini MA, Gouda EA (2021) Induction Motor Drive Using Fractional-Order Proportional Integral Derivative (FOPID) Controller Based on Nelder-Mead and Grey Wolf Optimizers. *MEJ-Mansoura Engineering Journal* 46: 23–31. https://doi.org/10.21608/bfemu.2021.178058
21. Swetha KT, Reddy BV, Jain RK (2022) A Direct Search Nelder Mead MPPT based Induction Motor Drive for Solar PV Water Pumping Systems. *2022 22nd National Power Systems Conference (NPSC)*, 578–583. https://doi.org/10.1109/NPSC57038.2022.10069049
22. Habbi F, Gabour NE, Bounekhla M, Boudissa EG (2021) Output voltage control of synchronous generator using Nelder–Mead algorithm based PI controller. *2021 18th International Multi-Conference on Systems, Signals & Devices (SSD)*, 365–374. https://doi.org/10.1109/SSD52085.2021.9429387
23. Mishra DD, Padhi P, Tripathy AA, Patnaik S, Sahoo PK (2023) Optimal Tuning of Fractional Order PID controller using Nelder-Mead Algorithm for DC Motor Speed Control. In *2023 International Conference in Advances in Power, Signal, and Information Technology (APSIT)*, 373–378. https://doi.org/10.1109/APSIT58554.2023.10201735
24. Mallik S, Mallik K, Barman A, Maiti D, Biswas SK, Deb Nk, et al. (2017) Efficiency and Cost Optimized Design of an Induction Motor Using Genetic Algorithm. *IEEE T Ind Electron* 64: 9854–9863. https://doi.org/10.1109/TIE.2017.2703687
25. Keskin B, Eminoğlu I (2022) Optimally Tuned PI Controller Design for V/f Control of Induction Motor. *2022 International Congress on Human-Computer Interaction, Optimization and Robotic Applications (HORA)*, 1–5. https://doi.org/10.1109/HORA55278.2022.9800005
26. Houili R, Hammoudi MY, Betka A, Titaouine A (2023) Stochastic optimization algorithms for parameter identification of three phase induction motors with experimental verification. *2023 International Conference on Advances in Electronics, Control and Communication Systems (ICAECCS)*, 1–6. https://doi.org/10.1109/ICAECCS56710.2023.10104526
27. Taradeh M, Mafarja M, Heidari AA, Faris H, Aljarah I, Mirjalili S, et al. (2019) An evolutionary gravitational search-based feature selection. *Inform Sciences* 497: 219–239. https://doi.org/10.1016/j.ins.2019.05.038
28. Jalil T, Boudour M, Tadjine M (2013) Optimal tuning of induction motor control using gravitational search algorithm. *2013 3rd International Conference on Systems and Control*, 208–213.

29. El Mahfoud M, Bossoufi B, El Ouanjli N, Said M, Taoussi M (2021) Improved direct torque control of doubly fed induction motor using space vector modulation. *Int J Intell Eng Syst* 14: 177–188. https://doi.org/10.22266/ijies2021.0630.16
30. El Ouanjli N, Mahfoud S, Al-Sumaiti AS, El Daoudi S, Derouich A, El Mahfoud M, et al. (2023) Improved twelve sectors DTC strategy of induction motor drive using Backstepping speed controller and P-MRAS stator resistance identification-design and validation. *Alex Eng J* 80: 358–371. https://doi.org/10.1016/j.aej.2023.08.077
31. El Idrissi A, Derouich A, Mahfoud S, El Ouanjli N, Chantoufi A, Al-Sumaiti AS, Mossa MA (2022) Bearing fault diagnosis for an induction motor controlled by an artificial neural network—Direct torque control using the Hilbert transform. *Mathematics* 10: 4258. https://doi.org/10.3390/math10224258
32. El Ouanjli N, Mahfoud S, Bhaskar MS, El Daoudi S, Derouich A, El Mahfoud M (2022) A new intelligent adaptation mechanism of MRAS based on a genetic algorithm applied to speed sensorless direct torque control for induction motor. *International Journal of Dynamics and Control* 10: 2095–2110. https://doi.org/10.1007/s40435-022-00947-z

AIMS Press